Strategies for the valorisation of a protein-rich saline waste stream into polyhydroxyalkanoates (PHA)

Alba Roibás-Rozas, Angeles Val del Rio, Almudena Hospido, Anuska Mosquera-Corral

Accepted manuscript

How to cite:

Bioresource Technology, 334 (2021), 124964. https://doi.org/10.1016/j.biortech.2021.124964

Strategies for the valorisation of a protein-rich saline waste stream into polyhydroxyalkanoates (PHA)

Alba Roibás-Rozas[1], Ángeles Val del Río, Almudena Hospido, Anuska Mosquera-Corral

CRETUS Institute, Department of Chemical Engineering, University of Santiago de Compostela, 15782, Santiago de Compostela, Galicia, Spain

Abstract

Saline Mussels Cooking Wastewater (MCW) was valorised to produce PHA with Mixed Microbial Cultures (MMC). Due to the high protein content (1.8 – 5.7 g COD_{PROT}/L), accumulating PHA capacity was initially below 10 %, so several strategies were tested to improve it. In the acidification unit Na(HCO_3) was added, which increased protein conversion to volatile fatty acids (VFA) from XX to XX %, while the accumulation PHA capacity increased from 6.9 to 14.7 %. In the enrichment unit the incorporation of a settling stage, after the feast phase, provoked a shift in the protein's oxidation from the feast to the famine phase, which is desirable because the nitrogen released in the famine is used by the MMC for growth, increasing the biomass concentration and the load treated (XX). The last strategy was to feed the enrichment unit with decreasing values of the proteins/VFA ratio, which allowed increasing the PHA accumulation from 8.8 to 41.5 %.

Keywords: Bioplastics; High salinity wastewater; Industrial Wastewater; Mixed Microbial Cultures; Protein-rich waste streams.

1. Introduction

[1] Corresponding author
e-mail: alba.roibas.rozas@usc.es (A. Roibás-Rozas)

PHA are renewable, biodegradable and bio-based polymers produced by bacteria which are expected to gradually replace conventional petrochemical plastics (Kourmentza et al., 2017). In the last decade, the use of mixed microbial cultures (MMC) and waste streams for PHA production has been explored to reduce overall costs and environmental impacts (Roibás-Rozas et al., 2020; Yadav et al., 2020). However, the use of waste streams for PHA production is challenging due to the complexity of the substrate, containing substances that can be inhibitory for the microbial activity (Korkakaki et al., 2016a; Palmeiro-Sánchez et al., 2019).The Spanish north-western region of Galicia is responsible for the 90 % of the production of mussels in the country, which is also the main mollusc producer of Europe (FAO, 2020). This activity generates more than 100 M€ of incomes and more than 10,000 jobs in the region (Rey-Méndez et al., 2016), and it is highly dependent on the water quality in the estuaries where seafood is harvested. Because of this, a proper treatment of the effluents generated in the fish-canning and fish-processing industries, normally located at shore areas, is essential for the environmental and economic preservation of the region. Nevertheless, the treatment of these effluents is challenging due to the presence of potentially inhibitory compounds, such as sodium chloride or ammonia. More precisely, the mussels cooking wastewater (MCW) contains high sodium chloride concentrations (between 17.9-19.0 g NaCl/L), as well as sulphate and nitrogen (organic and in the form of ammonia) in ranges that can be inhibitory for conventional processes, like the anaerobic digestion (Palmeiro-Sánchez et al., 2013). In fact, several attempts were made to valorise MCW in Galicia through biogas production. They were unsuccessful possibly due to the complexity of the waste stream (Barros et al., 2009; Omil et al., 1995), so the great concern regarding MCW treatment is reflected in local legislation

(Consellería de Medio Rural e Mar, 2015). Because of this, and its large biodegradable organic matter concentration, the valorisation of MCW by PHA production was defined as a possible alternative to treat these effluents. The Chemical Oxygen Demand (COD) of MCW, ranging between 9.8-26.5 g COD/L, is about 95 % soluble and mainly composed by proteins and carbohydrates. Carbohydrates are rapidly consumed in fermentation processes, but proteins are consumed slowly. Furthermore, their presence can provoke problems in the posterior aerobic PHA production units, so several strategies, as uncoupling the carbon and nitrogen feeding or introducing a settling stage in the process have been proposed (Argiz et al., 2020; Oliveira et al., 2017).

The aim of this research work is to evaluate how the presence of proteins affects the MMC-based PHA production process and to assess the feasibility of using protein-rich and saline wastewater as substrate. To do so, several long-term strategies were tested in a three-stage system for PHA production, using a MMC fed with MCW: i) alkalinity increase in the acidification unit; ii) settling stage in the PHA enrichment reactor; iii) and decreasing proteins/VFA ratio fed to acclimate the MMC in the enrichment unit. Then, these strategies were assessed and compared to choose the optimal operational conditions.

2. Material and methods

2.1 Experimental set-up

A three-step system was utilized to produce PHA (see Supplementary Material (SM)) as described in the following sections: a continuous stirred tank reactor (CSTR) for acidification of the MCW (2.1.1); a sequencing batch reactor (SBR) for enrichment of the MMC (2.1.2); and a fed batch reactor (FBR) for the accumulation of PHA (2.1.3).

The experimental stages tested in the continuous operation are summarized in Figure 1 and named as: A1-A6 for the acidification CSTR, E1-E5 for the enrichment SBR.

FIGURE 1 AROUND HERE

2.1.1 Continuously Stirred Tank Reactor (CSTR) for acidification

A CSTR was fed with MCW coming from a facility in Pontevedra, NW of Spain. Although the main compounds of the MCW did not change throughout the operational time, their concentrations fluctuated highly (see SM), so the Organic Loading Rate (OLR) for CSTR stages ranged between 1.01 and 1.76 g COD/(L·d). It had a volume of 5 L and it was operated as described in Fra-Vázquez et al. (2020). This study started in the operational day 400, where Volatile Fatty Acids (VFA) were produced steadily at a pH of 4.6 ± 0.6 with about 43 % of the effluent COD in the form of VFA. The Solid Retention Time (SRT) was fixed equal to the Hydraulic Retention Time (HRT), with a value of 6.25 days. The operational conditions by (Fra-Vázquez et al., 2020) were first maintained (stage A1), but then, different amounts of sodium bicarbonate were added (20 - 2700 mg $NaHCO_3$/L of MCW in stages A2 to A6, see Table 1) to increase the pH and improve protein solubility in the CSTR. The effluent produced in the CSTR was stored at 4 ºC until it was used in the following units. Therefore, operational stages for the CSTR and SBR (explained in section 2.1.2) were not synchronized, and their inter-relationship is also indicated in Table 1.

TABLE 1 AROUND HERE

2.1.2 Enrichment Sequencing Batch Reactor (SBR)

The inoculum of the SBR was enriched in PHA accumulating biomass (accumulation capacity of XX), as it came from a similar bench-scale reactor that was

fed with the same MCW for a year, but this feeding was diluted with tap water to decrease the salt concentration approximately to 5 g NaCl/L (Pedrouso et al. (2020)). For the present work, salinity was gradually increased until to achieve the salinity of the MCW (17-18 g NaCl/L) in 100 days by replacing the tap water by the effluent of the same SBR as dilution agent, which means that the SBR effluent was recirculated to the influent. Then, two different operational strategies (Cycles 1 and 2) were evaluated (see SM): conventional and modified Aerobic Dynamic Feeding (ADF and M-ADF, respectively). When the conventional ADF strategy (Cycle 1) was applied, air was continuously supplied while, with the M-ADF one (Cycle 2), a settling and discharge intermediate phases were included. In the case of Cycle 1, the exchanged volume was 50 % so the SRT and HRT of operation were equal to 1 day. For Cycle 2, no oxygen was supplied during the settling and supernatant discharge phases, and aeration was provided throughout the rest of the cycle phases. After settling, 25 % of the total reactor volume (V_R) was withdrawn (supernatant discharge), so during the rest of Cycle 2, the reactor operated with 75 % of the initial volume. As the initial feeding corresponded to 50 % of V_R and the final discharge was of 25 % of V_R, the SRT and HRT were of 2 and 1 days, respectively. The feeding of the SBR consisted of centrifuged CSTR effluent, where the dilution agent was the settled (without solids) effluent of the same SBR. The recirculation ratio (RR, i.e., volume of effluent from the CSTR / volume of effluent from the SBR used as feeding) was established according to the composition of the effluent produced in the CSTR and the organic load required to feed the SBR (Table 1). The operation of the SBR was divided in six stages (from E1 to E6) depending on the percentage of COD present as proteins (R_{PROT}) at the beginning of the cycles and on the cycle type (ADF or M-ADF) (Figure 1). Allylthiourea was added to the feeding of the

SBR at 10 mg/L to avoid nitrification, antifoaming (0.5 mL/L of feeding) to prevent spume problems and NaOH or HCl to maintain the pH value in the feeding approximately neutral in stages from E3 to E6, but pH inside the reactor was not controlled.

For all the stages, the reactor operated at 30 ºC by using a thermostatic bath (Techne Inc., USA), and air was supplied (6 L/min) through a ceramic air diffuser located at the bottom of the reactor. As the CSTR effluent was not enough to achieve the desired loads from stages E4 to E6, the SBR operation volume was reduced from 2 L (used from stages E1 to E3) to 1 L, maintaining all the operational conditions.

2.1.3 Accumulation Fed-Batch Reactor (FBR)

An FBR was employed to evaluate the maximal PHA accumulation capacity of the enriched MMC. As inoculum it was used the biomass from the SBR and as feeding the centrifuged effluent of the CSTR (containing VFA and the proteins) which was added in pulses. Analysis of the liquid phase (data no shown) showed that VFA were consumed first and proteins after, being possible to use the DO concentration value as indicator. For this reason, each pulse of feeding in the FBR was supplied when the DO concentration increased to intermediate values (approximately 4.0 - 4.5 mg O_2/L), which marked that VFA was depleted and protein oxidation started.

To make assays comparable, the amount of VFA supplied in every pulse was set as 15 $Cmmol_{VFA}/(L_{reactor} \cdot pulse)$. Except on day 388, when pulses of 70 $Cmmol_{VFA}/(L_{reactor} \cdot pulse)$ were used (increasing the volume of CSTR effluent in each pulse). Therefore, in the accumulation assays the volume of the FBR varied from 0.5 to 1.0 L, and the volume of the pulses changed according with the CSTR effluent

acidification degree, so the working volume of the FBR varied in the different experiments. Pulses were added until the accumulation assay achieved a maximum time of 12 hours, which equal the enrichment cycle length.

The reactor temperature was maintained at 30 °C by using a thermostatic bath (Techne Inc., USA), and air was supplied (6 L/min) through a ceramic air diffuser located at the bottom of the reactor.

2.2 Analytical methods

Conductivity and pH were measured with glass electrodes (Hach-Lange 50-60 and Crisson GLP22 respectively), while Dissolved Oxygen (DO) concentration and temperature were determined in the SBR and FBR with a probe (model HQ40d, Hach-Lange, USA). Alkalinity, Total Suspended Solids (TSS), Volatile Suspended Solids (VSS) and total COD (COD_T) concentrations were analysed in bulk samples, and the dissolved matter was characterised after filtering with a cellulose-ester filter of 0.45 μm pore size (Advantec, Japan), according to the Standard Methods (APHA-AWWA-WEF, 2017). Measuring included the following parameters: soluble COD (noted as COD in the text) carbohydrates, proteins, Total Organic Carbon (TOC), Total Nitrogen (TN), VFA, ammonium and other ions (Na^+, Cl^-, SO_4^{2-}). COD was generally quantified according to APHA-AWWA-WEF (2017), and based on the methodology described by Soto et al. (1989) when samples had concentrations below 5 g COD/L. Carbohydrates were measured as indicated in Dubois et al. (1956) and expressed as COD considering that 1 g of glucose (used as standard) corresponds to 1.07 g of COD. Proteins were analysed by the Lowry method (Lowry and Randall, 1951) and expressed as COD considering that bovine serum albumin (used as standard) contains 1.32 g of COD and

0.15 g of N per gram of protein. TOC and TN concentrations were measured by catalytic combustion in the TOC-L CNS analyser with the TNM-1 module (Shimadzu, Japan). VFA concentrations were determined in a gas chromatograph (Hewlett Packard 5890A, USA) equipped with a flame ionization detector (FID) and an automatic injector (Hewlett Packard 7673A, USA) and with ChemStation Rev. A. 10. 02 (1757) Agilent Thecnologies software. Ammonium was quantified by the Bower/Holm Hansen method (Bower and Holm-Hansen, 1980) and ions (Na^+, Cl^-, SO_4^{2-}) by ion chromatography (861 Advanced Compact IC, Metrohm, Switzerland).

PHA content was determined in biomass samples. To do so, unfiltered biomass samples were centrifuged, and the supernatant removed. Then, the remaining pellet was frozen and freeze-dried. The sample tube was weighed three times (empty, full of sample and after freeze-drying) to calculate the total solids in the pellet (TS). The PHA content (as g PHA/g VSS) was measured following the method described by Smolders et al. (1994) for the quantification of the monomer propyl esters present in a lyophilized sample. A commercial PHA standard (Sigma-Aldrich, USA) containing 88 % of hydroxybutyrate (HB) and 12 % of hydroxyvalerate (HV) and benzoic acid as internal standard were used. The propyl esters were analysed by means of gas chromatography in a HP innovax column equipped with an FID (Agilent, USA). Biogas composition (N_2, CH_4, CO_2, H_2S) was analyzed in a gas chromatograph (Hewlett Packard, USA) equipped with a packed column and a thermal conductivity detector (TCD) using helium as carrier gas and the percentage of each compound was calculated by analyzing 1 mL of biogas injected with a syringe.

2.3 Calculations

2.3.2 CSTR mass balances

For the CSTR, the main parameters calculated were the acidification degree (Ac., Eq. (1)), protein and carbohydrates removal percentages (REM_{CARB} and REM_{PROT}), Eq. (2)) and VFA production ($COD_{VFAprod}$, Eq. (3)). In Eq. (1), COD_{VFA} is the concentration of VFA in the effluent (g COD/L). Subindex i represents whether the equation refers to carbohydrates or proteins. "INF" and "EFF" subindexes represent influent and effluent streams, respectively.

$$Ac.(\%) = \frac{COD_{VFA}}{COD} \cdot 100 \quad (1)$$

$$REM_i(\%) = \frac{COD_{i,INF} - COD_{i,EFF}}{COD_{i,INF}} \cdot 100 \quad (2)$$

$$COD_{VFAprod} = \frac{COD_{VFA,EFF} - COD_{VFA,INF}}{COD_{INF}} \quad (3)$$

2.3.3 SBR mass balances

For the SBR, the COD concentration at the beginning of an enrichment cycle (COD_0, in g COD/L) was calculated according to eq. (4) because it has a 50 % of exchange volume ratio. Accordingly, the COD concentration of proteins or VFA at the beginning of the cycle ($COD_{i,0}$, g COD_i/L) was calculated as indicated in eq. (5). Analogously, this mass balance can be applied to calculate the concentration of the nitrogen forms in the cycle (substituting COD by TN or NH_4^+-N, in mg N/L). Here, "INF" refers to influent (feeding stream) and "EFF" to the effluent of the previous cycle, which coincides in concentration with the remaining volume inside the reactor. The proportion of COD_{PROT} or COD_{VFA} over the total COD at the beginning of the SBR cycles (R_i, % (g COD_i/g COD)) is calculated as stated in eq. (6). The COD in the feeding of the SBR is mainly due to the presence of VFA and proteins, therefore R_{VFA} in the SBR cycles is (1- R_{PROT}).

$$COD_0 = \frac{COD_{INF} + COD_{EFF}}{2} \quad (4)$$

$$COD_{i,0} = \frac{COD_{i,INF} + COD_{i,EFF}}{2} \quad (5)$$

$$R_i = \frac{COD_{i,0}}{COD_0} \cdot 100 \quad (6)$$

A mass balance was performed to calculate protein consumption during the cycle. For conventional ADF, protein removal is only due to oxidation. However, for Cycle 2 (M-ADF), protein removal also occurs due to the withdrawal of the supernatant. Therefore, the protein removal rate due to oxidation ($REM_{PROT,OX}$, %) and to supernatant removal ($REM_{PROT,SUP}$, %) is calculated according to eq. (7) and eq. (8), respectively, where V_{SUP} is the volume of the supernatant withdrawal and V_R is the reactor volume at the beginning of the cycle after feeding addition (section 2.1.2).

$$REM_{PROT,OX} = \frac{COD_{PROT,0} \cdot V_R - COD_{PROT,SUP} \cdot V_{SUP} - COD_{PROT,EFF} \cdot (V_R - V_{SUP})}{COD_{PROT,0} \cdot V_R} \cdot 100 \quad (7)$$

$$REM_{PROT,SUP} = \frac{COD_{PROT,SUP} \cdot V_{SUP}}{COD_{PROT,0} \cdot V_R} \cdot 100 \quad (8)$$

For Cycle 1, V_{SUP} is zero, so $REM_{PROT,OX}$ is ($COD_{PROT,0} - COD_{PROT,EFF}$)/$COD_{PROT,0}$. These mass balances can be applied for nitrogen forms by substituting COD_{PROT} by TN or NH_4^+-N. Finally, the protein variation during the cycle phases due to oxidation ($\Delta PROT_{OX}$ in g PROT/L) is calculated as indicated in eq. (9):

$$\Delta PROT_{OX} = \Delta PROT_F + \Delta PROT_{FAM} \quad (9)$$

Where $\Delta PROT_F$ and $\Delta PROT_{FAM}$ (both in g PROT/L) are the variation in the concentration of proteins during the feast and the famine phases, respectively, and they are calculated as indicated in eq. (10) and (11):

$$\Delta PROT_F = PROT_0 - PROT_{MID} \quad (10)$$

$$\Delta PROT_{FAM} = PROT_{EFF} - PROT_{MID} \quad (11)$$

Being $PROT_{MID}$ (g PROT/L) the protein concentration in the *middle* of the cycle (the point where feast finishes and famine begins). Accordingly, the percentage of COD_{PROT} oxidated during feast or famine ($REM_{PROT,F}$ or $REM_{PROT,FAM}$, in %) can be calculated by dividing $\Delta PROT_F$ or $\Delta PROT_{FAM}$ by $\Delta PROT_{OX}$ [2].

2.3.4 PHA content and consumption/production rates

For the SBR and the FBR, PHA content in the cells (as percentage) is calculated according to equation (12). Specific consumption and production rates (q_{VFA}, q_{PROT} and q_{PHA}, in mg/(g X·h)) are estimated from the maximum slopes of the curves obtained from the corresponding experimental data, divided by the average active biomass (X, calculated as the subtraction of the mass of PHA to the mass of VSS measured). The active biomass composition was considered $CH_{1.8}O_{0.5}N_{0.2}$ for all the calculations. The biomass yield (Y_X) was estimated dividing the biomass production rate (g COD_X/h) by the VFA consumption rate (COD_{VFA}/h). Finally, the ratio *r* (g VFA/g proteins) is calculated by dividing q_{VFA}/q_{PROT}.

$$PHA\ (wt.\%) = \frac{{}^{g\ TS}/_{L} \cdot {}^{g\ PHA\ in\ sample}/_{g\ TS}}{{}^{g\ VSS}/_{L}} \cdot 100 \qquad (12)$$

3. Protein fermentation in the acidification reactor (CSTR)

The CSTR operated for 621 days in 6 operational stages according to the $Na(HCO_3)$ added in the feeding, which was increased from 0 to 2,700 mg/L to improve proteins solubility and promote their better degradation. Changes in the applied load (1 - 1.76 g COD/(L·d)), are due to the variability of the MCW (Table 1). From stages A1 to

[2] Note that $REM_{PROT,F}$ and $REM_{PROT,FAM}$ (%) can be expressed as g/g or g COD_{PROT}/g COD_{PROT}, to obtain the same result.

238 A5, pH in the CSTR was always below 5.0 due to VFA formation and low alkalinity,
239 because the added amount of $Na(HCO_3)$ was still not enough to clearly increase the pH
240 value. For stage A6, pH was around neutrality (pH = 6.95 ± 0.57) due to the highest
241 added alkalinity dosage (2,700 mg $Na(HCO_3)$/L), so A6 corresponds to a neutral-pH
242 stage.

243 Carbohydrates were almost fully consumed (over 90 %) for every stage, but no
244 proteins (Figure 2). For acidic-pH stages (A1-A5) proteins removal ranged between
245 10.30 – 21.94 %, while for neutral-pH stage (A6) it increased to 42.45 ± 19.56 %. The
246 higher proteins removal promoted an increase in the $COD_{VFAprod}$ and acidification from
247 0.21 – 0.28 g COD_{VFA}/g COD and XX % (in A1-A5) to 0.43 ± 0.12 g COD_{VFA}/g COD
248 and 71.59 ± 13.05 % (in A6), respectively. Therefore, the increase in $COD_{VFAprod}$ and
249 acidification percentages for the neutral-pH stage can be attributed to the increase in the
250 protein consumption associated to the modified pH-environmental conditions.

251 Successful acidification of the MCW was achieved and no methane was detected
252 during the whole operational time. For stages A1-A5 (acidic-pH), the inhibition of
253 methanogenic activity can be attributed to the low pH of operation (below 5) caused by
254 VFA accumulation (Fra-Vázquez et al., 2020), but this cannot be the reason for the
255 inhibition for the neutral-pH stage (stage A6). Although high concentrations of salt, and
256 in special sodium ion, can inhibit methanogenic activity, methane can appear in long-
257 term operations despite high salinity (Palmeiro-Sánchez et al., 2013). However, when
258 sulphate is present in the wastewater and the COD/SO_4^{-2} ratio is below 10 g/g,
259 methanogens are inhibited due to their competition with sulphate reducing bacteria. In
260 this case, the complex matrix of MCW makes this waste stream ideal for VFA
261 production, as it has high concentrations of sodium due to salinity, and a COD/SO_4^{-2}

ratio below 10 g/g, which inhibits methanogens. Therefore, the compounds present in the MCW caused the absence of methanogenic activity during all the CSTR operation.

The transformation of proteins into VFA in anaerobic mixed culture fermentations has generated increasing interest in the last years (Bevilacqua et al., 2020; Jin et al., 2016; Liu et al., 2015; Regueira et al., 2020a, 2020b; Yang et al., 2015), as they are degraded slower than carbohydrates. Hydrolysates of proteins and carbohydrates are peptides/amino acids and glucose, respectively. As the presence of glucose represses protease formation, the uptake of glucose/carbohydrates happens first (Yang et al., 2015). Moreover, pH is one of the most relevant factors regarding VFA production from proteins (Regueira et al., 2020a). When pH is low and VFA are formed, undissociated acids cross the membrane, releasing protons inside the cell and inhibiting the generation of new acids. Furthermore, as the concentration of protons in the solution increases, the interaction of hydrogen bonds becomes stronger. Thus, the solubility of proteins decreases, as they aggregate and even coagulate at low pH values (Liu et al., 2015). This can explain the results of the CSTR operation, where carbohydrates are always consumed and proteins uptake only happens at the neutral-pH (stage A6).

FIGURE 2 AROUND HERE

4. Enrichment (SBR) and accumulation (FBR) reactors

The SBR was operated during 540 days, and the experimental time was divided in six stages (Figure 1), selected according to: a) CSTR operational conditions (generating an acidic-pH or neutral-pH feeding), b) proportion of COD_{PROT} in SBR cycles (if R_{PROT} is higher than 50 %, it is a high-COD_{PROT} stage; if R_{PROT} is below 50

285 %, it is a low-COD_{PROT} stage and, consequently, a high-COD_{VFA} stage), and c)
286 enrichment strategy (ADF or M-ADF). A recirculation was performed in four of the
287 stages (Table 1) with the aim of reaching stable salt concentrations avoiding the use of
288 tap water for dilution and load control. The maximum concentrations of 28.3 ± 0.7 g
289 NaCl/L in the SBR-FBR corresponded to the use of saline wastewater (19 g NaCl/L),
290 the addition of alkalinity as $Na(HCO_3)$, and NaOH for feeding pH control, so the raise
291 was gradual (data not shown) to let the biomass adapt to the highly saline conditions.

292 **4.1 SBR operation using acidic-pH feeding**

293 Proteins were always present in the SBR feeding, although their proportion
294 regarding the COD fed (R_{PROT}) varied (Figure 3a). To unravel the effect of proteins on
295 the enrichment process, two operational strategies were tested by applying the two
296 previously defined cycle distributions (ADF and M-ADF) to two levels of protein (high
297 and low R_{PROT}).

298 FIGURE 3 AND TABLE 2 AROUND HERE

299 **4.1.1. High R_{PROT} and conventional ADF**

300 The enrichment of PHA-accumulating organisms was initiated applying an ADF
301 regime (stage E1). Along with the 100 % consumption of VFA (data not shown),
302 approximately 34.7 % of the proteins were removed in each cycle during the feast
303 period (Table 2, Figure 3b). Therefore, the MMC consumed proteins simultaneously to
304 VFA. The presence of non-VFA COD in the enrichment process (like proteins) can be
305 harmful for the selection, as carbon is used by non-storing populations to grow and
306 proliferate in the system (Argiz et al., 2020). This issue was explored by (Korkakaki et
307 al., 2016b) for a system with methanol and VFA, where they proposed the parameter *r*

(q_{VFA}/q_{MeOH}) as a control for the enrichment success. They found that *r* needs to be equal to or higher than 4.7 g HAc/g MeOH (or 5 Cmol HAc/Cmol MeOH) for MMC selection to be effective. Here, *r* (q_{VFA}/q_{PROT}) had values of 0.81-2.60 g VFA/g protein (Table 2), indicating poor MMC selection, which in certain periods consumed proteins even faster than VFA. Hence, maximal PHA-accumulation capacities of the MMC from E1 in the FBR were always below 10 % (Table 2).

4.1.2. High R_{PROT} and M-ADF

Later, the cycle distribution of the SBR was modified to M-ADF (Stage E2), so a settling phase was introduced to improve MMC selection. After withdrawal the removed volume (which was 25 % of V_R) was not substituted with any other stream due to the inexistence of a current with the same composition of the acidified wastewater but without proteins, thus only 75 % of the initial volume remained inside the reactor during the rest of the cycle. Except for the beginning of E1, where the applied load was still being adapted, the SBR operated in E1 and E2 at similar COD_0 and $COD_{VFA,0}$ (Table 1, Figure 3a). For similar loads, *r* value generally increased from values below 3 g/g in E1, to values over 3 g/g in E2 (Table 2), indicating the MMC selection amelioration. Although the *r* value previously mentioned of 4.7 g HAc/g MeOH corresponded to a simple substrate (methanol), more complex substrates (as protein) could yield in a lower minimum *r* threshold.

Furthermore, a decrease in the protein oxidation by the MMC was observed with the change in the cycle type. Protein removal was about 35 % in E1, while it was around 47 % in E2. However, for E2, 20 % of the removal happened due to supernatant withdrawal, so oxidation by the MMC was only 27 %. Moreover, for E1, removal

happened basically during feast, while, for E2, proteins were consumed mostly during famine phase. Even so, the accumulation capacity of the MMC did not significantly increased in E2 (Table 2). It was observed that, when a high R_{VFA} (%) was applied to the SBR prior to the accumulation experiments in FBR (day 244 of operation), the MMC storing response improved. The accumulating capacity of the MMC in the FBR is highly dependent on the R_{VFA} (%) applied to the SBR: an R_{VFA} increase stimulate the storing response of MMCs (de Oliveira et al., 2019; Lorini et al., 2020). In fact, the accumulation capacity of the MMC in the FBR seemed to be boosted only by the R_{VFA} (g COD_{VFA}/g COD_0) of the SBR (Figure 4). Apparently, this behaviour is independent of the selection strategy applied (AFD, M-ADF).

FIGURE 4 AROUND HERE

On the other hand, the research studies carried out in the last years aim to incorporate the PHA production process in the wastewater treatment system to transform treatment lines into valorisation trains. Therefore, the production of PHA must be simultaneous to the removal of pollutants compounds. In this sense, the enrichment of the MMC can be simultaneous to processes involved in the biological nitrogen removal, like the partial nitritation (Fra-Vázquez et al., 2019), the nitritation/denitritation (Basset et al., 2016; Frison et al., 2015) or the denitrification (Santorio et al., 2019). Nevertheless, for carbonaceous compounds not useful for PHA production (like proteins), the preferred strategy consists of removing them from the system through a settling stage after the end of the feast phase which will also increase the concentration of storing populations (Argiz et al., 2020; Korkakaki et al., 2016b; Mulders et al., 2020). Moreover, when dealing with proteinaceous wastewater, it is also

common to remove them through other means prior to the enrichment process (Colombo et al., 2019).

Here, in stage E2, the MMC partially lost its capacity of consuming proteins. Hence, COD_{PROT} is present in the reactor outflows (supernatant and effluent streams, Figure 3b), meaning that, from a full-scale approach, further treatment would be needed before discharge. Uncoupling the carbon and nitrogen supply in the enrichment reactor has been successfully applied with protein-rich streams (Oliveira et al., 2017), but the supply of nitrogen is performed through the addition of chemicals, so the industrial application of this strategy can be hindered due to economic and environmental issues. Therefore, new strategies were tested to assess if PHA production and protein removal can occur in the same SBR cycle.

To do so, an strategy with decreasing proteins/VFA ratio fed was tested in E3. Here, the COD_0 was maintained in the same range as in E2, but the $COD_{VFA,0}$ was varied as follows: at the beginning of E3 (days 265 to 280), the feeding of the SBR consisted of raw MCW (non-acidified) and recirculated SBR effluent. Therefore, $COD_{VFA,0}$ was negligible, while the protein content was maintained at the same levels as in prior stages (Figure 3a). Then, raw MCW was gradually substituted by the fermented MCW coming from the CSTR, decreasing the proteins/VFA ratio. For E3, PHA accumulation increased in the SBR (below 10 % in E2, above 10 % in E3) along with protein oxidation (from 27 % in E2 to about 32 % in E3). Moreover, proteins were still consumed mainly in famine ($REM_{PROT,FAM}$ was 64.3 %, Table 2).

4.1.3. Low R_{PROT} and M-ADF

In stage E4 the CSTR effluent was directly fed to the SBR with no dilution, so R_{VFA} was higher than 50 % for the first time throughout the experimental period. The protein elimination in the SBR in this stage was about 72 %, with an 18 % due to the supernatant removal. Removal by oxidation (54 %) occurred in a 36 % in the feast and 64 % in the famine phases, so the protein consumption distribution in E4 were like that in E3 and E2 (mainly during famine). The PHA-storing capacities of the biomass in this stage were also the highest, exceeding the 40 % in the FBR and being of approximately 20 % in the SBR, with an *r* value of of 3.7 g/g. Therefore, proteins were consumed simultaneously to MMC enrichment in the SBR. The reached accumulation percentage (41.5 % of PHA in the FBR) exceeded the threshold value stablished for economic feasibility (Bengtsson et al., 2017), and it is similar to other results obtained in systems working with high proteins and/or salinity concentration. Hao et al. (2017) reported 42.3 % of PHA accumulation when they used fermented sludge with high protein content, and Wen et al. (2018) obtained 42.6 % of PHA when they employed fermented leachate at 15 g NaCl/L and 1.3 g COD/(L·d) in the SBR.

Besides, the biomass concentration was maximized, averaging 4.2 ± 1.8 g VSS/L in the SBR effluent, with the highest q_{PHA} and the lowest Y_X for all the stages tested (Table 2). When proteins were assimilated in stage E4, the total nitrogen consumption in SBR cycles (measured as the sum of organic and inorganic nitrogen forms, see SM) is higher than the apparent ammonium nitrogen consumption during the cycles. This indicates that the nitrogen released by the proteins is employed by the MMC for growth. So, as more nitrogen is available, the concentration of biomass increased to reach its highest value in E4 (Table 2), and higher organic loads are tolerated.

To the best of our knowledge, few works have explored the effect of proteins in enrichment reactors. Jia et al. (2013) fed an SBR for the enrichment of an MMC with simulated excess sludge fermentation liquid, so a mixture of synthetic VFAs was initially used. Then, bovine serum albumin was added to the SBR feeding to test its effect on the enrichment process. Although the addition of proteins worsened the enrichment performance, the results showed that its consumption during the cycle facilitated the cell growth. Moreover, a clear deterioration of the accumulation dynamic was found when R_{PROT} (g COD_{PROT}/g COD) was higher than 30 % in SBR feeding. Here, with the applied loads in stage E4, the R_{VFA} was 61.36 ± 9.97 %, and the best results were achieved in day 334, when R_{VFA} was as high as 69.9 % (so R_{PROT} was about 30 %). In fact, when Hao et al. (2017) used the guidance provided by Jia et al. (2013) to treat the excess sludge fermented liquid (containing proteins and carbohydrates), they achieved good results despite the presence of non-VFA organic matter.

Finally, Tu et al. (2020) harvested the biomass of a MMC in an enrichment reactor just after the feast phase. Then, the famine period was carried out in batch assays where different concentrations of non-VFA COD were added. In their study a worsening in the enrichment performance was detected, as internal PHA at the end of the cycle was higher than for cycles without addition of non-VFA COD. However, a lag phase in the profile of PHA consumption of the stored carbon was detected in the MMC while non-VFA COD was consumed. This suggested that the microorganisms capable of storing PHA can also choose the substrate to be consumed (internal or external) when both are available.

Therefore, although high concentrations of proteins are harmful for the accumulation process (above 30 % of the COD), their presence can stimulate the system dynamics, as proteins are non-VFA COD, but they are also nitrogen and carbon sources. Moreover, protein consumption releases nitrogen, that will be used by the two present populations (storing and non-storing) for growth in the famine phase. Consequently, proteins can enhance the process performance if a dynamic balance is stablished in the reactor medium and if proper acclimation and selection strategies are applied as demonstrated here.

Consequently, the imposed enrichment strategy (ADF or M-ADF) is not directly responsible of an increase in the MMC accumulating capacity. However, the imposition of a proper selection dynamic and of a second selective pressure (the settling stage) is necessary to increase the applied load that will rise the storing response. Moreover, the presence of proteins can be beneficial for the system if R_{VFA} is about 70 %, as the released nitrogen due to protein uptake can be used by biomass for growth. As more biomass is available, the tolerated loads will be higher and PHA production can be increased.

Finally, because of the optimized behaviour in the system, two different accumulation approaches were tested as indicated in Section 2.1.3. The best results were obtained when 15 Cmmol/(L·pulse) were applied (day 334) (Table 2).

4.2 SBR operation using neutral-pH feeding

4.2.1 High R_{PROT} and M-ADF

The proteins present in the SBR feeding in stage E5 were the ones not transformed into VFA in the CSTR in A6 (operated at 6.25 days of residence time and

446 neutral pH), so proteins were less available for the MMC. Because of this, when the
447 applied loads of E4 were tested in E5 (COD_0 was 4 – 5 g COD/L, Figure 3a), the feast
448 phase lasted 6-8 hours (feast length lasted about 2.75 hours for steady operation, see
449 SM), and the biomass concentration in the reactor decreased to 2.7 ± 1.1 g VSS/L
450 (Table 2). Due to this instability, accumulation cycles could not be performed and, to
451 attain steady state conditions, the applied load was diminished down to reach a COD_0 of
452 2 – 3 g COD/L and R_{PROT} increased due to recirculation. When no proteins are
453 available, the selection of the MMC is supposed to be improved, as the concentration of
454 non-VFA forms of COD decreases. However, as less nitrogen is available, less growth
455 is promoted so the biomass concentration at the end of the cycle decreases, and organic
456 load needs to be reduced to maintain the accumulation dynamic.

457 In stage E5, the value of *r* increased to its highest level basically because
458 proteins were slightly consumed. However, PHA storing decreased to 14.03 % in the
459 SBR since the applied load could not be raised due to excessively length of the feast
460 periods (6-8 hours) and the occurrence of the biomass loss. Moreover, q_{PHA} for the
461 enrichment cycles in the stage E5 presented the lowest values of any tested stage of 8.9
462 mg PHA/(g X·h) and protein oxidation decreased to 28.2 %. Nevertheless, it still
463 happened during the famine phase (like in the other stages with M-ADF).

464 **4.2.1 High R_{PROT} and ADF**

465 In stage E6, the settling phase was removed from the cycle and the ADF strategy
466 was imposed as in the stage E1. Here, although protein removal due to oxidation
467 decreased to 23.5 %, the accumulation in the SBR and FBR worsened to values of

468 5.09 % and 14.66 %, respectively. Moreover, protein consumption occurred during the
469 feast phase for the two stages where conventional ADF was tested (E1 and E6, Table 2).

470 Generally, when proteins are consumed during the feast phase of the cycle, the
471 enrichment process is unsuccessful (Korkakaki et al., 2016b; Oliveira et al., 2017).
472 Although their presence is normally considered undesirable, protein consumption
473 during the famine stage can promote biomass growth without negatively affecting the
474 enrichment performance when its presence is lower than 30 % of the COD (Jia et al.,
475 2013). In the present study, although the enrichment strategy did not directly affect the
476 accumulating capacity for the same applied loads, it had clear and significant impact on
477 the protein consumption profile. For the stages with ADF strategy (only relying on the
478 FF regime), proteins were totally or mainly consumed during the feast phase of the
479 cycle, but, when the M-ADF strategy was imposed, they were consumed mostly during
480 the famine phase. Therefore, M-ADF improved the culture selection, while protein
481 consumption during famine was linked to an increase in the concentration of
482 accumulating microorganisms. Finally, as storing populations proliferated and biomass
483 concentration was higher, the tolerated loads and the PHA accumulation raised.

484 Summing up, the enrichment strategy did not directly affect the storing capacity
485 (it is only boosted by the load increase), but it does indirectly as a load raise is only
486 possible if a proper enrichment strategy (M-ADF) is applied. Therefore, proper
487 selection of the culture (where non-VFA forms are present) is only possible if two
488 selective pressures are imposed.

489 Again, the maximum COD_0 tolerated by the system was 2 – 3 g COD/L, so
490 R_{PROT} increased due to dilution. Moreover, a change in the enrichment strategy reversed

491 the SBR behaviour, which presented similar *r* values and biomass concentration than in
492 stage E1, while protein oxidation occurred again during famine (as in E1, Table 2).
493 Therefore, for the same operational strategy but lower protein availability, the system
494 performance was not improved in E5 although protein consumption was lower with
495 respect to stage E1.

496 **5. Conclusion**

497 Proteins conversion into VFA in the acidification unit was enhanced from XX
498 to XX % with the addition in the feeding of $Na(HCO_3)$ to have neutral pH. In the
499 enrichment unit, proteins can be beneficial (at concentrations below 30 % of COD) if
500 the enrichment strategy includes a settling stage to promote their consumption in the
501 famine, because nitrogen is released and used for biomass growth. Therefore, as
502 biomass concentration increases, the load tolerated and the amount of PHA produced by
503 the system are higher. Finally, the decrease of the proteins/VFA ratio to acclimate the
504 MMC to proteins, allowed increasing the PHA accumulation from 8.8 to 41.5 %.

505

506 E-supplementary data of this work can be found in online version of the paper.

507 **6. Acknowledgements**

508 This research was supported by the Spanish Government (AEI) through
509 TREASURE [CTQ2017-83225-C2-1-R] project. The authors belong to a Galician
510 Competitive Research Group (GRC). The programme is co-funded by the FEDER (EU).
511 Icons made by www.flaticon.com. Mar Orge and Mónica Dosil are acknowledged for
512 their support on analytical methods.

7. Author contributions

Alba Roibás-Rozas: Formal analysis, Investigation, Writing – original draft, Conceptualization, Resources. **Ángeles Val del Río:** Validation, Writing - review & editing, Visualization, Conceptualization, Funding acquisition, Supervision **Anuska Mosquera-Corral**: Conceptualization, Validation, Resources, Writing - review & editing, Supervision, Project administration, Funding acquisition. **Almudena Hospido**: Writing - review & editing, Supervision, Project administration, Funding acquisition.

8. References

1. APHA-AWWA-WEF, 2017. STANDARD METHODS FOR THE EXAMINATION OF WATER AND WASTEWATER, 23RD EDITION. American Public Health Association/American Water Works Association/Water Environment Federation, Washington DC, USA.
2. Argiz, L., Fra-Vázquez, A., Val del Río, Á., Mosquera-Corral, A., 2020. Optimization of an enriched mixed culture to increase PHA accumulation using industrial saline complex wastewater as a substrate. Chemosphere 247. https://doi.org/10.1016/j.chemosphere.2020.125873
3. Barros, M.C., Magán, A., Valiño, S., Bello, P.M., Casares, J.J., Blanco, J.M., 2009. Identification of best available techniques in the seafood industry: a case study. J. Clean. Prod. 17, 391–399. https://doi.org/10.1016/j.jclepro.2008.08.012
4. Basset, N., Katsou, E., Frison, N., Malamis, S., Dosta, J., Fatone, F., 2016. Integrating the selection of PHA storing biomass and nitrogen removal via nitrite in the main wastewater treatment line. Bioresour. Technol. 200, 820–829. https://doi.org/10.1016/j.biortech.2015.10.063
5. Bengtsson, S., Werker, A., Visser, C., Korving, L., 2017. PHARIO Stepping stone to a sustainable value chain for PHA bioplastic using municipal activated sludge.
6. Bevilacqua, R., Regueira, A., Mauricio-Iglesias, M., Lema, J.M., Carballa, M., 2020. Protein composition determines the preferential consumption of amino acids during anaerobic mixed-culture fermentation. Water Res. 183, 115958. https://doi.org/10.1016/j.watres.2020.115958

7. Bower, C.E., Holm-Hansen, T., 1980. A Salicylate–Hypochlorite Method for Determining Ammonia in Seawater. Can. J. Fish. Aquat. Sci. 37, 794–798. https://doi.org/10.1139/f80-106
8. Colombo, B., Villegas Calvo, M., Pepè Sciarria, T., Scaglia, B., Savio Kizito, S., D'Imporzano, G., Adani, F., 2019. Biohydrogen and polyhydroxyalkanoates (PHA) as products of a two-steps bioprocess from deproteinized dairy wastes. Waste Manag. 95, 22–31. https://doi.org/10.1016/j.wasman.2019.05.052
9. Consellería de Medio Rural e Mar, 2015. DOG nº 21. Galicia.
10. de Oliveira, G.H.D., Niz, M.Y.K., Zaiat, M., Rodrigues, J.A.D., 2019. Effects of the Organic Loading Rate on Polyhydroxyalkanoate Production from Sugarcane Stillage by Mixed Microbial Cultures. Appl. Biochem. Biotechnol. 189, 1039–1055. https://doi.org/10.1007/s12010-019-03051-9
11. Dubois, M., Gilles, K.A., Hamilton, J.K., Rebers, P.A., Smith, F., 1956. Colorimetric Method for Determination of Sugars and Related Substances. Anal. Chem. 28, 350–356. https://doi.org/10.1021/ac60111a017
12. FAO, 2020. GLOBEFISH - Information and Analysis on World Fish Trade [WWW Document]. Eur. Mark. mussels. URL http://www.fao.org/in-action/globefish/fishery-information/resource-detail/en/c/338588/ (accessed 7.22.20).
13. Fra-Vázquez, A., Pedrouso, A., Val del Rio, A., Mosquera-Corral, A., 2020. Volatile fatty acid production from saline cooked mussel processing wastewater at low pH. Sci. Total Environ. 732, 139337. https://doi.org/10.1016/j.scitotenv.2020.139337
14. Fra-Vázquez, A., Santorio, S., Palmeiro-Sánchez, T., Val del Río, Á., Mosquera-Corral, A., 2019. PHA accumulation of a mixed microbial culture co-exists with ammonia partial nitritation. Chem. Eng. J. 360, 1255–1261. https://doi.org/10.1016/j.cej.2018.10.207
15. Frison, N., Katsou, E., Malamis, S., Oehmen, A., Fatone, F., 2015. Development of a Novel Process Integrating the Treatment of Sludge Reject Water and the Production of Polyhydroxyalkanoates (PHAs). https://doi.org/10.1021/acs.est.5b01776
16. Hao, J., Wang, X., Wang, H., 2017. Overall process of using a valerate- dominant

574 sludge hydrolysate to produce high-quality polyhydroxyalkanoates (PHA) in a
575 mixed culture 1–11. https://doi.org/10.1038/s41598-017-07154-3
576 17. Jia, Q., Wang, H., Wang, X., 2013. Dynamic synthesis of polyhydroxyalkanoates
577 by bacterial consortium from simulated excess sludge fermentation liquid.
578 Bioresour. Technol. 140, 328–336.
579 https://doi.org/10.1016/j.biortech.2013.04.105
580 18. Jin, B., Wang, S., Xing, L., Li, B., Peng, Y., 2016. The effect of salinity on waste
581 activated sludge alkaline fermentation and kinetic analysis. J. Environ. Sci. 43,
582 80–90. https://doi.org/10.1016/j.jes.2015.10.011
583 19. Korkakaki, E., Mulders, M., Veeken, A., Rozendal, R., van Loosdrecht,
584 M.C.M.M., Kleerebezem, R., 2016a. PHA production from the organic fraction
585 of municipal solid waste (OFMSW): Overcoming the inhibitory matrix. Water
586 Res. 96, 74–83. https://doi.org/10.1016/j.watres.2016.03.033
587 20. Korkakaki, E., van Loosdrecht, M.C.M., Kleerebezem, R., 2016b. Survival of the
588 fastest: Selective removal of the side population for enhanced PHA production in
589 a mixed substrate enrichment. Bioresour. Technol. 216, 1022–1029.
590 https://doi.org/10.1016/j.biortech.2016.05.125
591 21. Kourmentza, C., Plácido, J., Venetsaneas, N., Burniol-Figols, A., Varrone, C.,
592 Gavala, H.N., Reis, M.A.M., 2017. Recent advances and challenges towards
593 sustainable polyhydroxyalkanoate (PHA) production. Bioengineering 4, 1–43.
594 https://doi.org/10.3390/bioengineering4020055
595 22. Liu, X., Hu, X., Wang, J., Song, Y., Wang, M., Liu, R., Duan, L., 2015. Evaluating
596 properties of protein in waste activated sludge for volatile fatty acid production:
597 effect of pH. Environ. Earth Sci. 73, 5047–5056. https://doi.org/10.1007/s12665-
598 015-4194-0
599 23. Lorini, L., di Re, F., Majone, M., Valentino, F., 2020. High rate selection of PHA
600 accumulating mixed cultures in sequencing batch reactors with uncoupled carbon
601 and nitrogen feeding. N. Biotechnol. 56, 140–148.
602 https://doi.org/10.1016/j.nbt.2020.01.006
603 24. Lowry, O.H., Randall, R.J., 1951. Protein Measurement byt the Folin Reagent. J.
604 Biol. Chem. 193, 265–275. https://doi.org/10.1016/0304-3894(92)87011-4
605 25. Mulders, M., Tamis, J., Abbas, B., Sousa, J., Dijkman, H., Rozendal, R.,

606 Kleerebezem, R., 2020. Pilot-Scale Polyhydroxyalkanoate Production from
607 Organic Waste: Process Characteristics at High pH and High Ammonium
608 Concentration. J. Environ. Eng. (United States) 146, 1–11.
609 https://doi.org/10.1061/(ASCE)EE.1943-7870.0001719
610 26. Oliveira, C.S.S., Silva, C.E., Carvalho, G., Reis, M.A., 2017. Strategies for
611 efficiently selecting PHA producing mixed microbial cultures using complex
612 feedstocks: Feast and famine regime and uncoupled carbon and nitrogen
613 availabilities. N. Biotechnol. 37, 69–79. https://doi.org/10.1016/j.nbt.2016.10.008
614 27. Omil, F., Méndez, R., Lema, J.M., 1995. Anaerobic treatment of saline
615 wastewaters under high sulphide and ammonia content. Bioresour. Technol.
616 https://doi.org/10.1016/0960-8524(95)00143-3
617 28. Palmeiro-Sánchez, T., Val Del Rio, A., Fra-Vázquez, A., Luis Campos, J.,
618 Mosquera-Corral, A., 2019. High-Yield Synthesis of Poly(3-hydroxybutyrate- co-
619 3-hydroxyvalerate) Copolymers in a Mixed Microbial Culture: Effect of Substrate
620 Switching and F/M Ratio. Ind. Eng. Chem. Res. 58, 21921–21926.
621 https://doi.org/10.1021/acs.iecr.9b03514
622 29. Palmeiro-Sánchez, T., Val del Río, A., Mosquera-Corral, A., Campos, J.L.,
623 Méndez, R., 2013. Comparison of the anaerobic digestion of activated and aerobic
624 granular sludges under brackish conditions. Chem. Eng. J. 231, 449–454.
625 https://doi.org/10.1016/j.cej.2013.07.052
626 30. Pedrouso, A., Fra-vazquez, A., Val, A., Mosquera-Corral, A., 2020. Recovery of
627 Polyhydroxyalkanoates from Cooked Mussel Processing Wastewater at High
628 Salinity and Acidic Conditions. Sustainability 12.
629 https://doi.org/10.3390/su122410386
630 31. Regueira, A., Bevilacqua, R., Lema, J.M., Carballa, M., Mauricio-Iglesias, M.,
631 2020a. A metabolic model for targeted volatile fatty acids production by
632 cofermentation of carbohydrates and proteins. Bioresour. Technol. 298, 122535.
633 https://doi.org/10.1016/j.biortech.2019.122535
634 32. Regueira, A., Lema, J.M., Carballa, M., Mauricio-Iglesias, M., 2020b. Metabolic
635 modeling for predicting VFA production from protein-rich substrates by mixed-
636 culture fermentation. Biotechnol. Bioeng. 117, 73–84.
637 https://doi.org/10.1002/bit.27177

638 33. Rey-Méndez, M., Fernández Casal, J., Lodeiros, C., Guerra, A., 2016. XVIII Foro
639 dos recursos mariños e da acuicultura das rías galegas. Santiago de Compostela.
640 34. Roibás-Rozas, A., Mosquera-Corral, A., Hospido, A., 2020. Environmental
641 assessment of complex wastewater valorisation by polyhydroxyalkanoates
642 production. Sci. Total Environ. 744.
643 https://doi.org/10.1016/j.scitotenv.2020.140893
644 35. Santorio, S., Fra-Vázquez, A., Val del Rio, A., Mosquera-Corral, A., 2019.
645 Potential of endogenous PHA as electron donor for denitrification. Sci. Total
646 Environ. 695. https://doi.org/10.1016/j.scitotenv.2019.133747
647 36. Smolders, G.J.F., van der Meij, J., van Loosdrecht, M.C.., Heijnen, J.., 1994.
648 Stoichiometric model of the aerobic metabolism of the biological phosphorus
649 removal process. Biotechnol. Bioeng. 44, 837–848.
650 https://doi.org/https://doi.org/10.1002/bit.260440709
651 37. Soto, M., Veiga, M.C., Méndez, R., Lema, J.M., 1989. Semi-micro C.O.D.
652 determination method for high-salinity wastewater. Environ. Technol. Lett. 10,
653 541–548. https://doi.org/https://doi.org/10.1080/09593338909384770
654 38. Tu, W., Zou, Y., Wu, M., Wang, H., 2020. Reducing the effect of non-volatile
655 fatty acids (non-VFAs) on polyhydroxyalkanoates (PHA) production from
656 fermented thermal-hydrolyzed sludge. Int. J. Biol. Macromol. 155, 1317–1324.
657 https://doi.org/10.1016/j.ijbiomac.2019.11.103
658 39. Wen, Q., Ji, Y., Hao, Y., Huang, L., Chen, Z., Sposob, M., 2018. Effect of sodium
659 chloride on polyhydroxyalkanoate production from food waste fermentation
660 leachate under different organic loading rate. Bioresour. Technol. 267, 133–140.
661 https://doi.org/10.1016/j.biortech.2018.07.036
662 40. Yadav, B., Pandey, A., Kumar, L.R., Tyagi, R.D., 2020. Bioconversion of waste
663 (water)/residues to bioplastics- A circular bioeconomy approach. Bioresour.
664 Technol. 298, 122584. https://doi.org/10.1016/j.biortech.2019.122584
665 41. Yang, G., Zhang, P., Zhang, G., Wang, Y., Yang, A., 2015. Degradation
666 properties of protein and carbohydrate during sludge anaerobic digestion.
667 Bioresour. Technol. 192, 126–130.
668 https://doi.org/10.1016/j.biortech.2015.05.076
669

TABLES AND FIGURES

Table 1: Operational Stages throughout the operation of the acidification (CSTR) and the enrichment units (SBR).

Table 2: Main results obtained by the monitoring of operational cycles in the enrichment and accumulation reactors.

Figure 1: Operational stages in the three-stage PHA production system. Continuous lines represent the operational stages and dashed lines represent the mass balances for each stage. The boxes filled with diagonal grey lines for the enrichment stages represent the periods where the volume of the reactor was reduced from 2 L to 1 L. fMCW is the acidified effluent of the Continuously Stirred Tank Reactor (CSTR).

Figure 2: Protein Removal (REM_{PROT}, □), carbohydrates removal (REM_{CARB}, ■), and Acidification Degree (Ac, Δ), expressed as percentages, and VFA production ($COD_{VFAprod}$ ○, g COD_{VFA}/g COD_{INF}) in the CSTR.

Figure 3: a) COD concentration at the beginning of SBR cycles: COD_0 (○), $COD_{VFA,0}$ (■) and $COD_{PROT,0}$ (●), in g COD/L. b) Protein concentration in SBR: in the influent

693 ($COD_{PROT,INF}$ ♦), at the beginning of the cycle ($COD_{PROT,0}$, ●), in the supernatant

694 ($COD_{PROT,SUP}$, Δ), and in the effluent ($COD_{PROT,EFF}$ □), expressed as g COD_{PROT}/L.

695 Figure 4: Relationship between R_{VFA} (%) in the SBR and the stored PHA (%) in the

696 FBR, for experiments without settling (Cycle 1, ADF) (○) and with settling phase

697 (Cycle 2, M-ADF) (●).

Table 1

Acidification Reactor (CSTR)					Enrichment Reactor (SBR)						
Stage	**Na(HCO_3) (mg/L of feeding)**	**Days**	**OLR (g COD/(L·d))**	**Stage in SBR[a]**	**Stage**	**Days**	**Cycle**	**$COD_{VFA,0}$ (g COD_{VFA}/L)**	**R_{VFA}, % (g COD_{VFA}/g COD)**	**SRT (days)**	**RR[b]**
A1	0	0-263	1.01 ± 0.21	E1-E2	E1	0-205	ADF	0.50 ± 0.26	34.98 ± 16.79	1	1:4
A2	20	264-332	1.27 ± 0.13	E2-E2a	E2	206-263	M-ADF	0.71 ± 0.11	32.02 ± 7.32	2	1:5
A3	80	333-395	1.44 ± 0.23	E3	E2a	264-335	M-ADF	0.72 ± 0.32	33.19 ± 14.22	2	1:6 to 1:1
A4	320	396-466	1.76 ± 0.21	E3	E3	336-425	M-ADF	2.69 ± 0.75	61.36 ± 9.97	2	1:1 or 1:0
A5	640	467-502	1.75 ± 0.21	E4	E4	425-498	M-ADF	1.75 ± 0.48	51.28 ± 8.84	2	1:1 to 1:3
A6	2700	503-621	1.48 ± 0.42	E4-E5	E5	499-536	ADF	0.94 ± 0.37	36.98 ± 4.73	1	1:4

[a] CSTR effluent was stored until used, so the operational time is not always coincident. This column shows the link between the effluents obtained in each acidification CSTR operational stage (employed as SBR feeding) and the SBR operational stage.

[b] RR: Recirculation ratio to the SBR (CSTR effluent volume : SBR recirculated effluent volume).

Table 2

Stage	**E1** (ADF)				**E2** (M-ADF)			**E3** (M-ADF)		**E4** (M-ADF)		**E5** (M-ADF)	**E6** (ADF)
Protein removal in SBR: total, due to oxidation ($REM_{PROT,OX}$) **and due to supernatant withdrawal** ($REMP_{PROT,SUP}$)													
Average Total Protein Removal[(1)]	34.7				47.4			46.3		71.8		52.9	23.5
Oxidation (%)	34.7				27.0			31.9		53.6		28.2	23.5
Withdrawal (%)	-				20.4			14.4		18.1		24.8	-
Protein oxidation distribution over the enrichment cycles: during feast ($REM_{PROT,OX,F}$) **and during famine** ($REM_{PROT,OX,FAM}$)													
Feast (%)	98.2				25.7			35.7		37.1		0.0	100.0
Famine (%)	1.8				74.3			64.3		62.9		100.0	0.0
Biomass concentration at the end of SBR cycles													
Biomass (g VSS/L)	1.3 ± 0.7				2.5 ± 0.5			1.6 ± 0.4		4.2 ± 1.8		2.7 ± 1.1	1.4 ± 0.2
CYCLES													
SBR													
Day	11	88	123	187	228	244	255	302	318	349		473	513
PHA (%)	12.4	11.5	3.5	3.6	5.4	8.2	6.7	14.6	11.0	18.8		14.0	5.1
q_{PHA} (mg PHA/(g X·h))	18.5	24.7	20.5	49.8	27.5	49.9	37.3	-	-	21.68		8.9	14.0
r (q_{VFA}/q_{PROT}), g/g	1.5	2.6	0.81	1.3	6.0	6.0	3.2	-	-	3.7		36.2	1.5
FBR													
Day	97		139		236	250	257			334	388		508
PHA (%)	**6.9**		**7.8**		**7.3**	**17.8**	**8.8**			**41.5**	**28.6**		**14.7**
q_{PHA} (mg PHA/(g X·h))	13.2		10.0		13.9	6.3	17.2			68.1	36.9		24.5
Y_X (g COD_X/g COD_{VFA})	14.2		49.2		49.5	33.3	31.2			1.4	1.8		9.2
CONDITIONS OF SBR CYCLE PREVIOUS TO THE FBR-ACCUMULATION ASSAY													
COD_0 g COD/L	2.0		2.5		2.5	2.0	2.1			3.6	5.3		2.6
R_{VFA} (%)	19.1		31.9		29.6	46.6	29.9			69.9	58.0		37.8

[(1)] The average protein removal is calculated using the protein concentration measured twice weekly in the SBR streams during each operational stage. The protein oxidation taking place in the feast or famine phases is calculated using the data obtained in the cycles monitored monthly throughout the operational time. Standard deviations of the elimination percentages are not provided because the wastewater composition was highly variable, so the propagation of uncertainty due to this variability generated extremely high and non-representative dispersions.

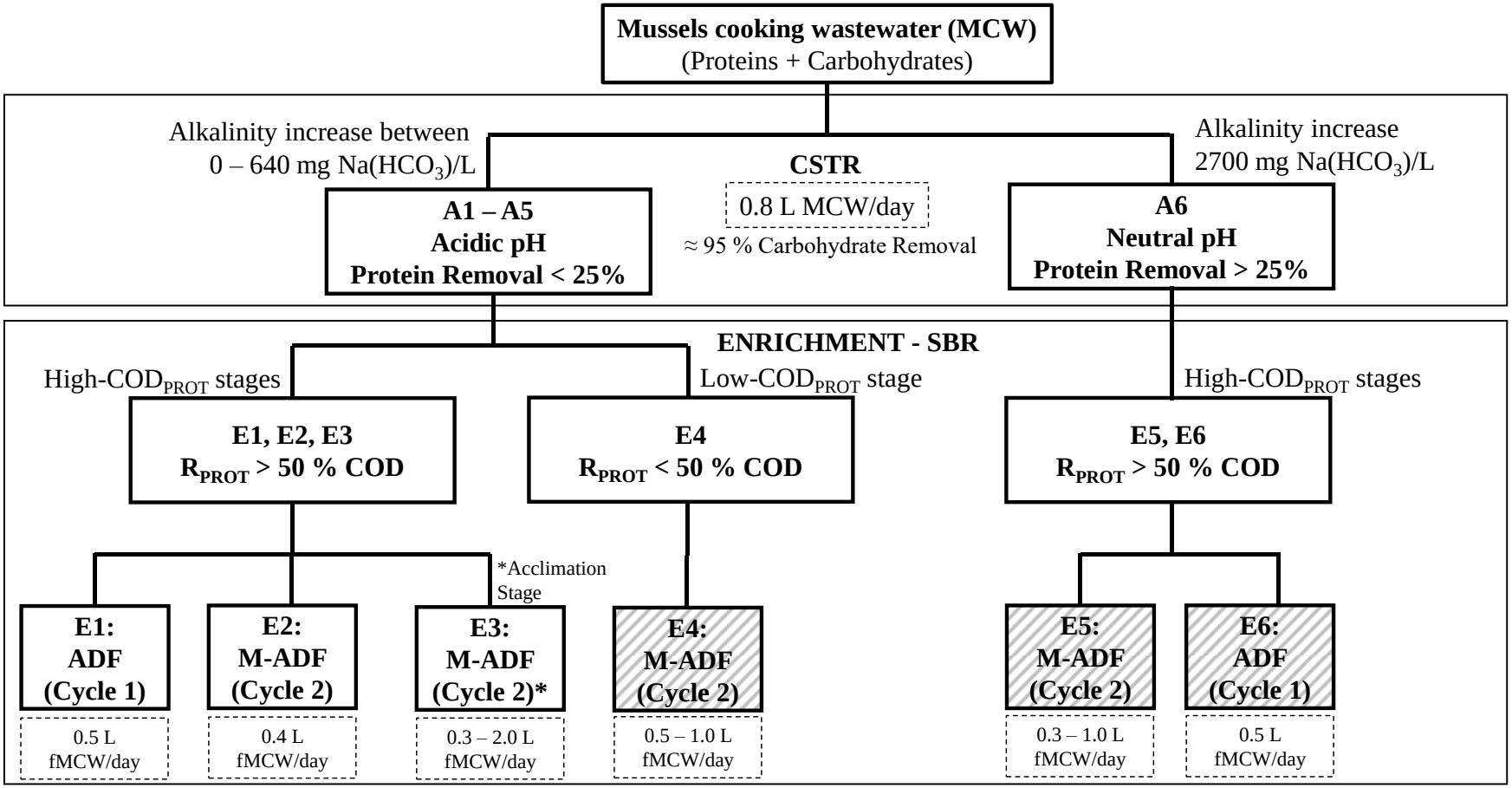
Mussels cooking wastewater (MCW)
(Proteins + Carbohydrates)
Alkalinity increase between
0 – 640 mg Na(HCO3)/L
CSTR
0.8 L MCW/day
≈ 95 % Carbohydrate Removal
Alkalinity increase
2700 mg Na(HCO3)/L
A1 – A5
Acidic pH
Protein Removal < 25%
A6
Neutral pH
Protein Removal > 25%
ENRICHMENT - SBR
High-CODPROT stages
Low-CODPROT stage
High-CODPROT stages
E1, E2, E3
RPROT > 50 % COD
E4
RPROT < 50 % COD
E5, E6
RPROT > 50 % COD
*Acclimation
Stage
E1:
ADF
(Cycle 1)
E2:
M-ADF
(Cycle 2)
E3:
M-ADF
(Cycle 2)*
E4:
M-ADF
(Cycle 2)
E5:
M-ADF
(Cycle 2)
E6:
ADF
(Cycle 1)
0.5 L
fMCW/day
0.4 L
fMCW/day
0.3 – 2.0 L
fMCW/day
0.5 – 1.0 L
fMCW/day
0.3 – 1.0 L
fMCW/day
0.5 L
fMCW/day

Figure 1

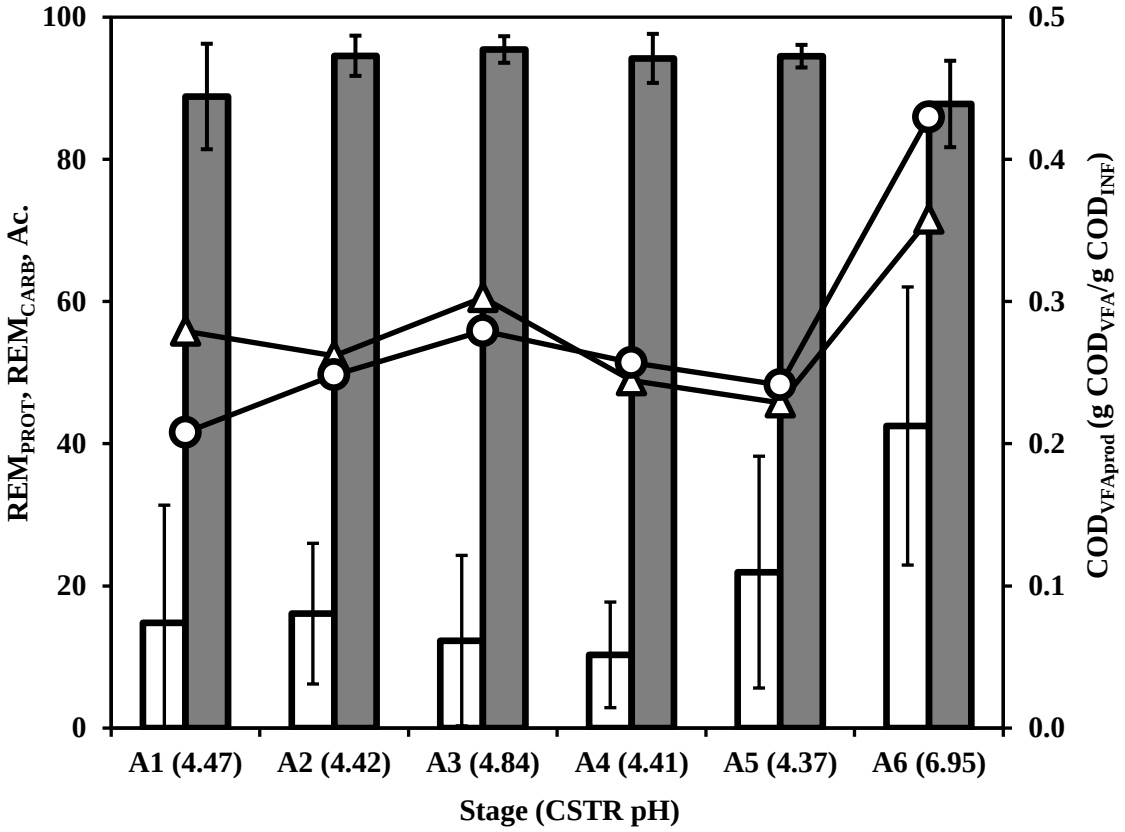
100
80
60
40
20
0
0.5
0.4
0.3
0.2
0.1
0.0
REMPROT, REMCARB, Ac.
CODVFAprod (g CODVFA/g CODINF)
A1 (4.47)
A2 (4.42)
A3 (4.84)
A4 (4.41)
A5 (4.37)
A6 (6.95)
Stage (CSTR pH)

Figure 2

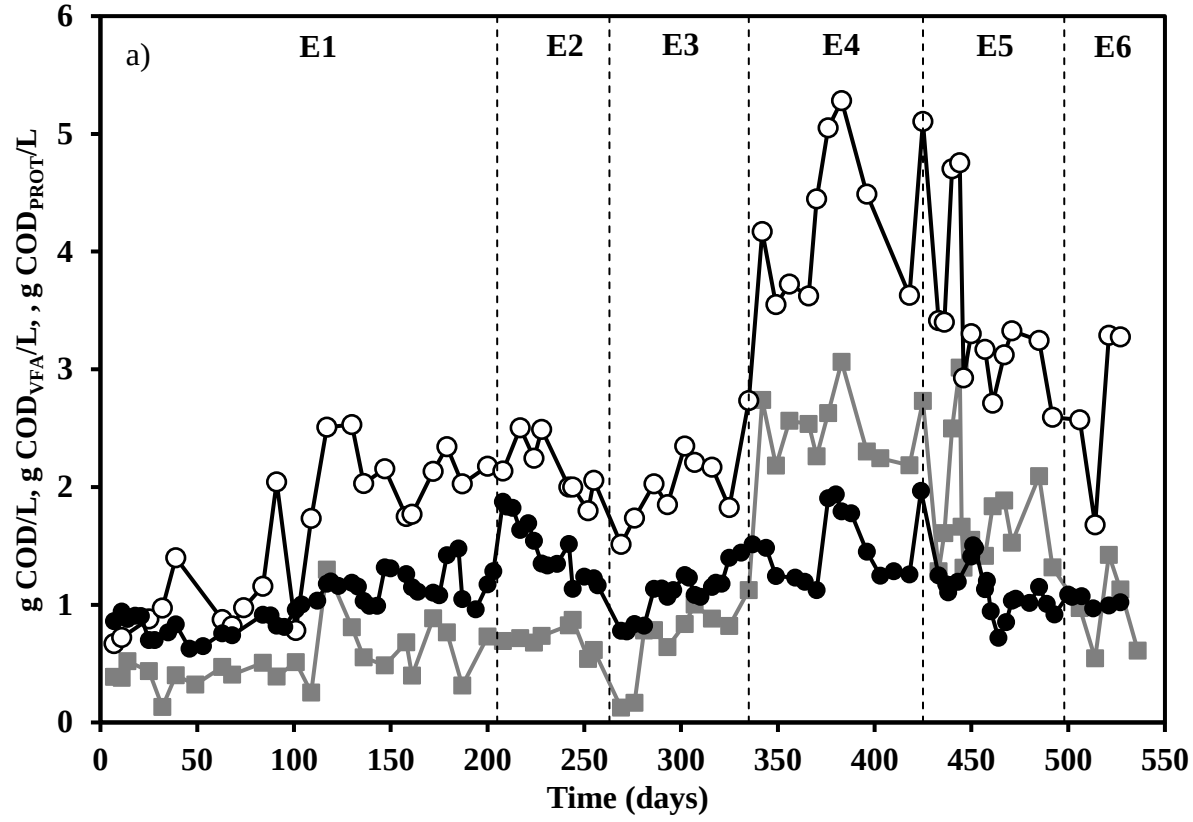

736

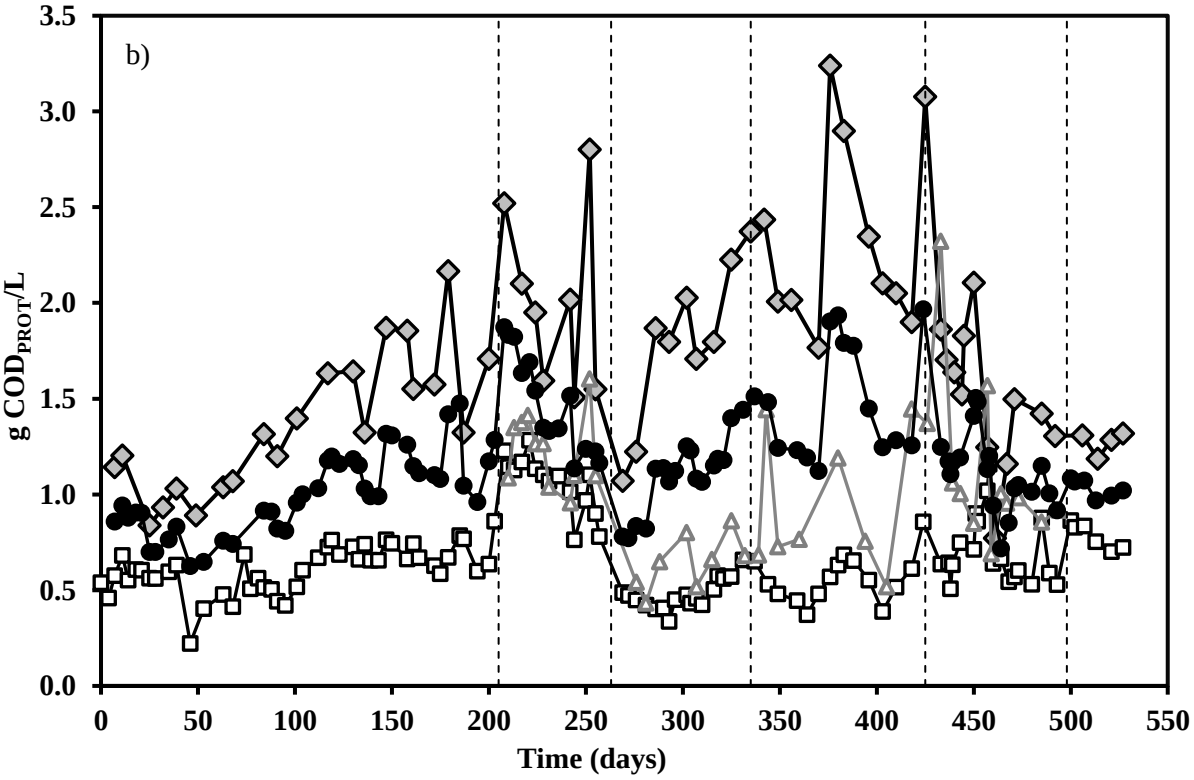

737

738 **Figure 3**

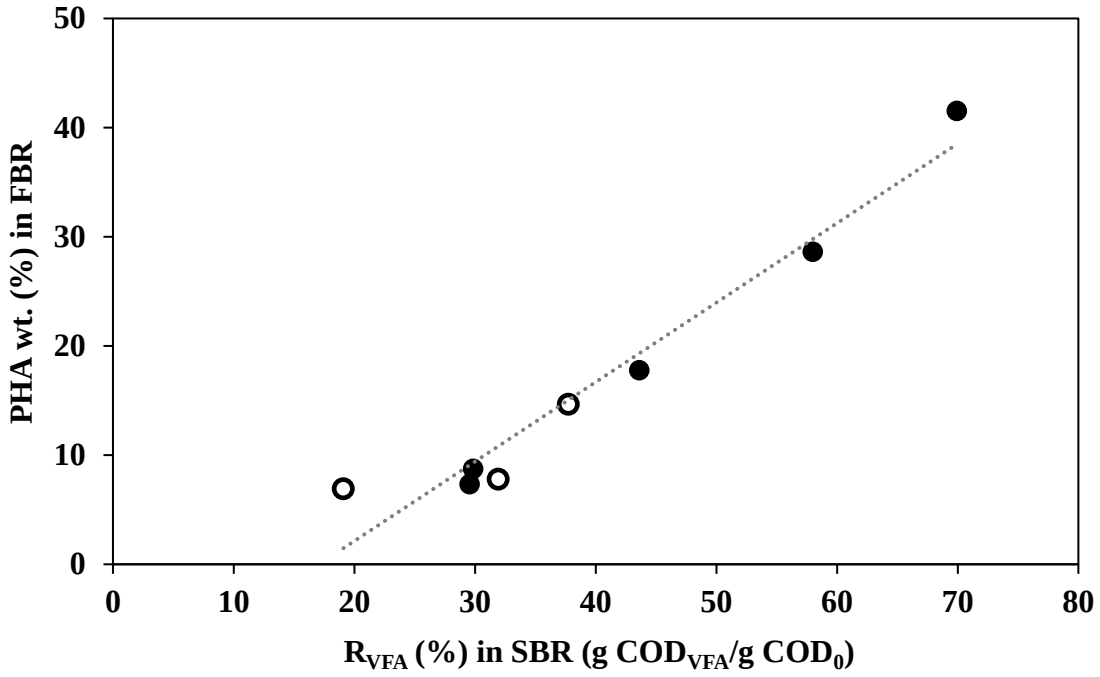

739

740 **Figure 4**

741